Organic & Biomolecular Chemistry

PAPER

View Article Online
View Journal

Cite this: DOI: 10.1039/c9ob00058e

Enhancing the kinetics of hydrazone exchange processes: an experimental and computational study†

Patrick L. Higgs, [a] Antonio J. Ruiz-Sanchez, [a] Milene Dalmina, [a] Benjamin R. Horrocks, [a] Andrew G. Leach *[b] and David A. Fulton *[a]

The capacity of hydrazone bonds to readily undergo component exchange processes sees their extensive utilization in dynamic combinatorial chemistry. The kinetics of hydrazone exchange are optimal at pH ~4.5, which limits the use of hydrazone-based dynamic combinatorial libraries, particularly for biological targets which are only stable at near-neutral pH values. It would thus be advantageous if hydrazone exchange proceeded with faster rates at pH values closer to neutral. We experimentally and computationally evaluated the hypothesis that hydrazones possessing neighbouring acidic or basic functional groups within the carbonyl-derived moitety of the hydrazone would enhance exchange rates. Our work suggests that judiciously placed *N*- or *O*-hydrogen bond acceptors within the carbonyl-derived moiety of the hydrazone stabilize transition states *via* hydrogen bonding interactions, providing a valuable boost to exchange kinetics at near-neutral pH values. We anticipate these findings will be of interest in dynamic combinatorial chemistry, dynamic covalent polymers/materials, functionalized nanoparticles and interlocked molecules, all of which may benefit from hydrazone exchange processes able to operate at near-neutral pH values.

Received 9th January 2019,
Accepted 25th February 2019

DOI: 10.1039/c9ob00058e

rsc.li/obc

Introduction

The field of dynamic combinatorial chemistry[1] requires chemical bonds that readily undergo component exchange processes. One of the most utilized is the hydrazone bond, (Fig. 1) which has optimal exchange kinetics at pH 4.5, being considerably slower at neutral pH.[1b,2] The requirement to operate at lower pH limits significantly the scope and application of hydrazone-based dynamic combinatorial libraries as many interesting biological templates are only stable at near neutral pH values, and thus it would be advantageous if hydrazone exchange were able to operate on an experimentally useful timescale at pH values closer to neutral.

Inspired by the work[3] of Jencks in the 1960s, Dawson and co-workers demonstrated[4] that aniline can successfully catalyse exchange processes at neutral pH, and aniline catalysis was applied[5] successfully in a hydrazone-based dynamic combinatorial library for the discovery of inhibitors of glutathione *S*-transferase. The relatively high concentrations of aniline required (100 mM) to enhance the rate of component exchange can limit significantly the wider biocompatibility of the organocatalyst approach, and to this end Kool *et al.* have developed[6] improved catalysts which can provide rate enhancements of up to eight times that of aniline catalysis at lower concentrations of catalyst.

While investigating hydrazone and oxime formation at neutral pH, Kool and co-workers also studied[6a] an alternative approach to organocatalysis in which structural modifications of aldehyde components can increase the rate of hydrazone or oxime formation at neutral pH. These structural modifications involve the inclusion of neighbouring acidic or basic functional groups or atoms within the carbonyl-derived moiety of the hydrazone that assist proton transfer within the rate limiting step, thus lowering transition state energies and enhancing the rate of hydrazone formation. We reasoned that these structural modifications may also help increase the rate of hydrazone exchange processes at neutral pH. Thus, in this work, we

Fig. 1 Hydrazones undergo reversible component exchange through transimination processes where a hydrazone reacts with a hydrazide to afford a new hydrazone and hydrazide.

[a]Chemical Nanoscience Laboratory, Chemistry-School of Natural and Environmental Sciences, Bedson Building, Newcastle University, Newcastle upon Tyne, NE1 7RU, UK. E-mail: david.fulton@ncl.ac.uk; Tel: +44(0)191 208 7065
[b]School of Pharmacy and Biomolecular Sciences, James Parsons Building, Liverpool John Moores University, Byrom Street, Liverpool, L3 3AF, UK.
E-mail: A.G.leach@ljmu.ac.uk; Tel: +44(0)151 231 2404

†Electronic supplementary information (ESI) available. See DOI: 10.1039/c9ob00058e

investigated exchange kinetics for a small pool of hydrazones containing acidic or basic functional groups/atoms and rationalized their observed order of reactivity by computational studies. Our computational model indicates that the rate enhancements likely arise on account of the abilities of neighbouring functional groups/atoms to form stabilizing hydrogen bonds within the transition state. Furthermore, this model correctly identified benzodihydropyran (benzoDHP) as a candidate rate-enhancing group – a prediction that was initially surprising given the absence of any acidic or basic moieties within benzoDHP – which was verified by experiment to be the fastest performing group, demonstrating that useful enhancements in rate can be obtained.

Results and discussion

Experimental hydrazone exchange studies

When considering the application of hydrazone bonds in dynamic combinatorial chemistry, one must take account of several important requirements. It is crucial that equilibria lie very much on the side of product hydrazone, and thus aromatic aldehyde partners are often used as the extended conjugation of the resultant hydrazone ensures product stability, especially important when operating in aqueous solutions. Aliphatic aldehydes, on the other hand, tend to form hydrazones where the equilibrium is less towards the desired hydrazone. Furthermore, acyl hydrazide reaction partners are used to ensure reasonable rates of component exchange as other classes of hydrazides/hydrazines often form hydrazones which undergo component exchange on too slow a timescale to be useful. With these considerations in mind, we focused upon a small pool of hydrazones **1a–f** (Fig. 2) (for synthetic procedures see ESI†).

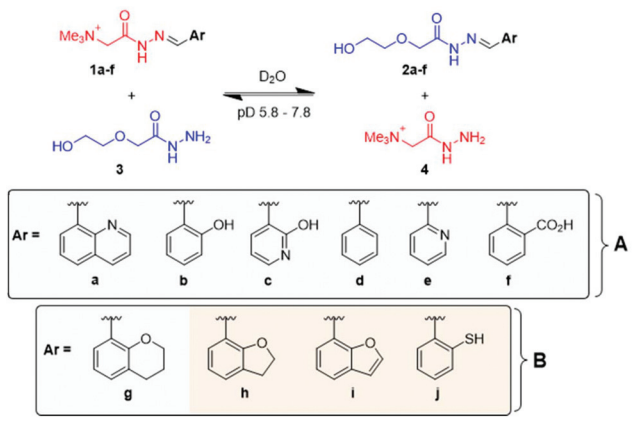

Fig. 2 Component exchange of hydrazones **1a–f** with acyl hydrazide **3** to form hydrazones **2a–f** and acyl hydrazide **4**, a process which was studied by ^{1}H NMR spectroscopy. (A) Exchange of **1a–f** was studied both experimentally and modelled computationally as a symmetrical exchange process, where $AcNHNH_2$ is both the attacking nucleophile, and hydrazide component of the hydrazone. (B) Substrates **h–j** were only studied computationally, and based upon the outcomes of this work, **g** was progressed to experimental study.

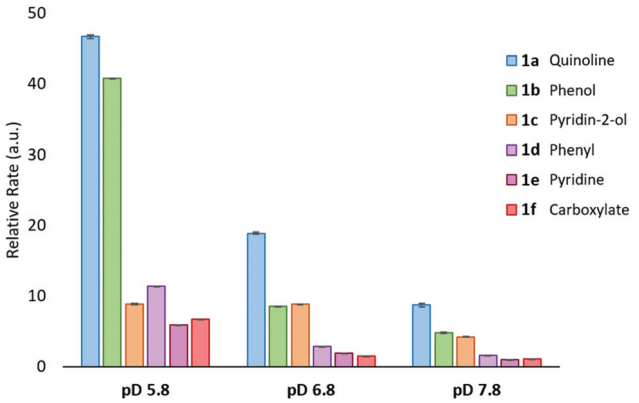

Fig. 3 Relative rates of component exchange for hydrazones **1a–f**, which were obtained from the forward rate constant values k_f (see ESI† for details). Error bars show $\pm$ 1σ confidence intervals.

Hydrazones **1a–c** and **1e–f** contain a basic nitrogen or acidic group either upon or within the aromatic moiety of the carbonyl components which we postulated would likely influence the kinetics of exchange. These specific substrates were chosen based upon the work[6a] of Kool *et al.*, where they displayed relatively high rate enhancements for hydrazone formation and thus are sensible starting points to investigate their influence on hydrazone exchange. Hydrazone **1d** contains no potential rate-enhancing structural features, and thus serves as a control.

Component exchange to form hydrazones **2a–f** was accomplished by reaction of hydrazones **1a–f** with an excess of acyl hydrazide **3** (see ESI† for experimental details). Acyl hydrazides **3** and **4** possess hydroxyl and quaternary ammonium groups, respectively, which ensure water solubility of their associated hydrazones. Exchange reactions (see ESI† for details) were monitored by ^{1}H NMR spectroscopy at room temperature over a range of pD values (5.4–7.4).‡ The mole fraction of each species in solution was determined at each time point from the normalized integrals of diagnostic protons. We found any diagnostic signal could be used as a spectral handle to quantify the rate of component exchange, and for experimental simplicity we chose to utilize signals associated with hydrazones **1a–f** and exchange product **4** (Fig. 2). ^{1}H NMR spectroscopic integral analysis afforded kinetics traces (see ESI, Fig S10†) from which the second order rate constants (k_f and k_r) were determined (see ESI† for details), allowing for the relative rates of hydrazone exchange (Fig. 3) to be deduced.

As anticipated, the kinetics of exchange of all examples were faster as the pD decreased. The rates of exchange are 2–8 times faster at the lowest pD investigated (5.4) compared to the highest pD (7.8), observations consistent with component exchange being accelerated by protonation. Component

‡All experimental studies are performed in D_2O and thus acidities were measured in pD. Computational studies which were modelled in H_2O with acidity measured in pH. pD can be related to pH by the simple calculation pD = pH + 0.42.[21]

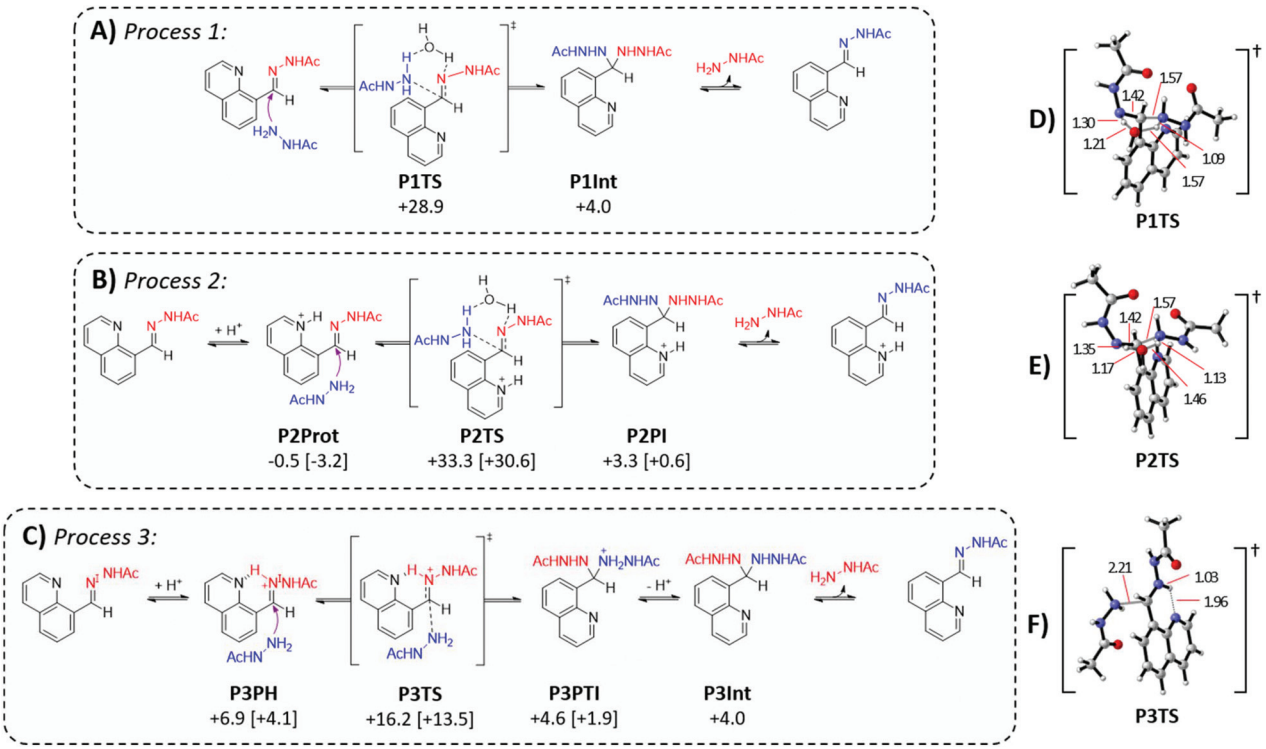

Fig. 4 Three mechanisms of hydrazone exchange which were explored computationally. (A) Process (1): No protonation of hydrazone prior to hydrazide attack (uncatalysed reaction). (B) Process (2): Protonation of proximal acid/base group within aldehyde component of hydrazone prior to attack. (C) Process (3): Protonation of hydrazone nitrogen (N^{I}) prior to attack. Energetics (kcal mol^{-1}) were calculated at pH 7, whilst values for pH 5 are in brackets. Process (3) represents the most likely mechanism for hydrazone exchange, on account of having low energy barriers, relative to Processes (1) and (2). (D–F) Transition state structures **P1TS**, **P2TS** and **P3TS**, respectively.

exchange was fastest with hydrazone **1a**, being approximately 5 times faster than control hydrazone **1d** at all pD values investigated, suggesting that the inclusion of a proximal basic nitrogen may catalyse hydrazone exchange. Surprisingly, hydrazones **1e** and **1f** – both of which possess proximal acid/basic groups – were observed to undergo slower component exchange processes (at all pD values) than the control hydrazone **1d**. This result was initially surprising as we had anticipated that the hydrazone containing the most basic group would best catalyse the hydrazone exchange process as it would exhibit the greatest likelihood of being protonated and so be able to transfer a proton in the rate limiting step; the pK_a of the pyridyl nitrogen is estimated to be 5.14,[7] which is higher than that of the quinoline (pK_a = 4.85)[7] and the benzoic acid (pK_a = 4.20)[7] suggesting that pyridine **1e** should undergo the fastest hydrazone exchange. Our observed order of reactivity (quinoline > phenol > phenyl > pyridine ≈ carboxylate) does not correlate with the pK_a value of the proximal acid/basic groups, an observation which suggests that the rate enhancement is not caused by protonation of this group.

Computational hydrazone exchange studies

In order to better understand our experimental observations, computational studies were undertaken. To the best of our knowledge, this is the first computational study to explicitly examine the mechanism of hydrazone exchange. Three possible hydrazone exchange mechanisms were considered and studied at the M06-2X/6-31G* level[8] of theory (a level that is expected to produce reasonable agreement with barrier heights). All calculations were performed in Gaussian09[9] and included implicit solvation using the PCM protocol.§ To simplify calculations, the hydrazide employed in modelling the exchange processes was $AcNHNH_2$, which was also used as the hydrazide component within the hydrazone. The overall process modelled was therefore a symmetrical exchange. We considered firstly process (1) (Fig. 4A) in which no protons were added into the system. In the calculated transition state (**P1TS**), proton shuttling between the incoming nucleophile and the hydrazone was required, and a single water molecule can fulfill this role by simultaneously removing a proton from the incoming hydrazine and protonating the hydrazone. This proton shuttling leads to a neutral tetrahedral intermediate (**P1Int**) that would be expected to collapse either to reactants or products through similar barriers. In process (2) (Fig. 4B), groups located within the aldehyde-derived moiety of the hydrazone were protonated to give reaction precursors (**P2Prot**) before nucleophilic attack by the hydrazide, a process that pro-

§ All species were characterized by frequency calculations.

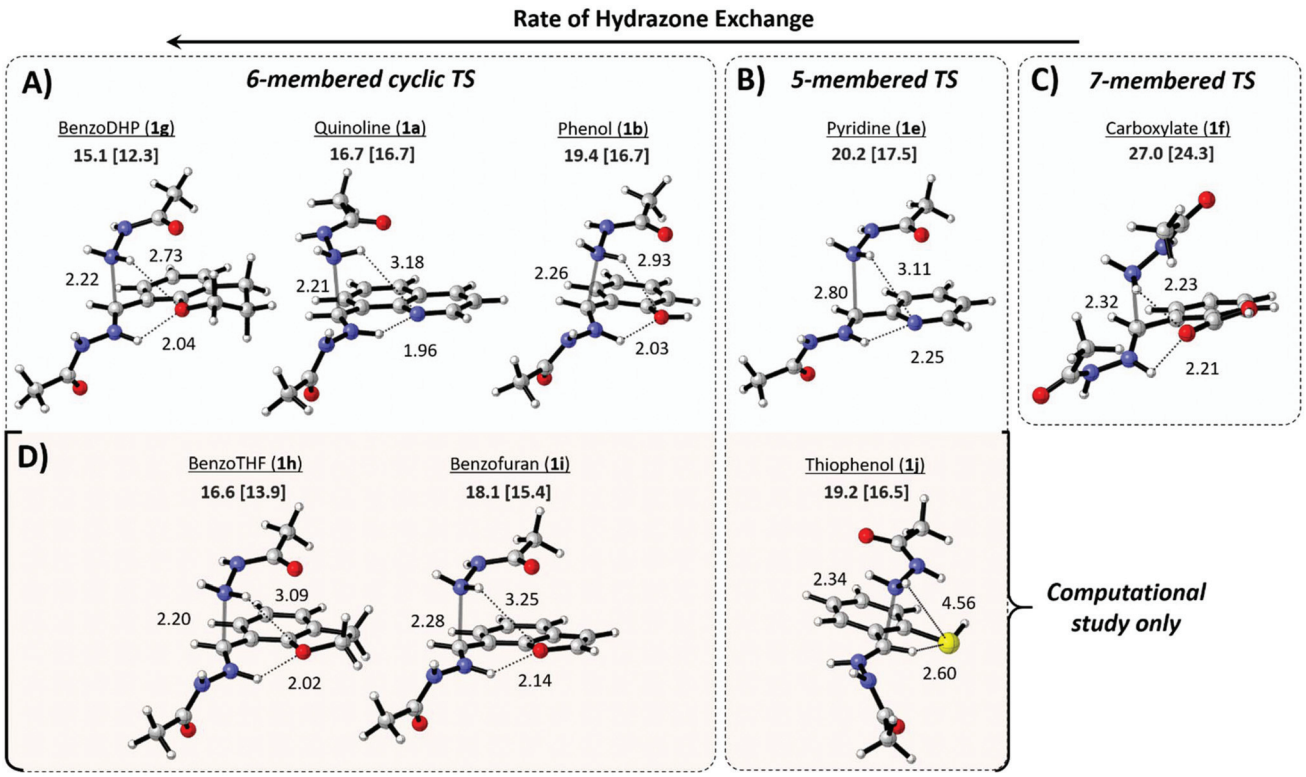

Fig. 5 Hydrogen bonding interactions stabilise the transition states for hydrazone exchange. The energy barriers ($\Delta G^{\dagger}$) corresponding to each TS structure were calculated at pH 7.4 and pH 5.4 (brackets). (A) 6-membered cyclic TS (benzoDHP **1g**, quinoline **1a**, phenol **1b**) have the lowest energies and exhibit the fastest hydrazone exchange. (B) 5-membered cyclic TS (pyridine **1c**, thiophenol **1j**), 7-membered TS (carboxylate **1f**). (D) Substrates **1h–j** were only studied computationally.

ceeds through a similar transition state (**P2TS**) to process (1). This mechanism leads to a protonated intermediate (**P2PI**) that can either rearrange (intramolecular proton transfer) or return a proton to the surrounding environment. The computed energetics (see $\Delta G^{\dagger}$ values in Fig. 4) are those calculated for pH 7, while those for pH 5 (where different) are in brackets. The calculated values reveal that process (2) features a high energy barrier, with $\Delta G^{\dagger}$ values exceeding 30 kcal mol^{-1}, indicating that protonation of the functional group/atom within the aldehyde-derived moiety likely impedes the exchange process. We then considered process (3) (Fig. 4C), which represents a specific acid-catalysed reaction in which hydrazone nitrogen (N^1) is protonated prior to nucleophilic attack by the hydrazide. This protonation gives protonated hydrazone (**P3PH**) that is attacked by hydrazide through transition state **P3TS** to give a protonated tetrahedral intermediate **P3PTI**. For process (3) the calculated free energy barrier (see $\Delta G^{\dagger}$ values) is significantly lower than those obtained for processes (1) and (2), indicating that process (3) constitutes the most likely mechanism for hydrazone exchange. The pathway with the lowest free energy barrier is likely to be the one that is operational but there are significant uncertainties in these comparisons and therefore the ability of each process to explain the relative reactivity of the different hydrazones was also considered.

For process (1), the lowest computed free energy barrier (and therefore fastest reaction) is for carboxylate **1f**¶ (see ESI, Table S19†) whilst the highest energy process (and therefore slowest) involves quinoline **1a**, observations that are not consistent with experiment and therefore process (1) was discounted. The energetics calculated for process (2) (ESI, Table S20†) predict that: (i) the most reactive substrate is control compound **1d** – which is absent of any acid/basic groups to catalyse the reaction; and (ii) the least reactive substrate is **1a** – which was experimentally observed to have the fastest hydrazone exchange kinetics. Process (2) was not consistent with the observed order of reactivity and was discounted. The computed barrier heights for process (3) (ESI, Table S21†) however, predict an order of reactivity (pH 7.4: **1a** > **1b** > **1d** ≈ **1e** > **1f**; pH 5.4: **1a** ≈ **1b** > **1d** ≈ **1e** > **1f**) that was consistent with the observed relative rates (Fig. 3), further sup-

¶Further modelling of **1f** revealed that the carboxylate moiety may ring-close upon the aminal-like intermediate to form a meta-stable 5-membered cyclic structure (Fig. S24†), although no evidence of this species was observed during ^{1}H NMR experiments. This meta-stable presented a local minimum on the potential energy surface, making it challenging to reliably compute energetics that were consistent with a single exchange mechanism. Energetics of all other substrates however, were in close agreement with process (3).

porting the idea that process (3) constitutes the most likely mechanism of hydrazone exchange.

We then further scrutinized the key species that governs reactivity *via* process (3), the transition state for hydrazide attack (**P3TS**). The origin of the high reactivity of **1a** was revealed in the corresponding transition state structure (Fig. 5A), which features two hydrogen bonds from the quinoline nitrogen to both the incoming hydrazide (N–H distance: 3.18 Å) and the protonated hydrazone (N–H: 1.96 Å), that stabilize the transition state.[10] Crucially, these stabilizing interactions help to lower the energy barrier for hydrazone exchange, thus providing a boost in the exchange kinetics. In the analogous transition states for pyridine **1e** (N–H: 3.11 Å, 2.25 Å) and carboxylate **1f** (O–H: 2.23 Å, 2.21 Å) (Fig. 5B and C) these distances are longer, suggesting that of the two interactions it is the hydrogen bond to the protonated hydrazone that governs reactivity. It has been noted previously[11] that 6-membered ring intramolecular hydrogen bonding interactions (such as those that operate for quinoline **1a**) are slightly favoured over their 5-membered equivalent (as for pyridine **1e**) and much favoured compared to their 7-membered equivalent (carboxylate **1f**). Thus, it is the ideal spatial positioning and orientation of hydrogen bond acceptor atoms/groups within the transition state, rather than simply the presence of acidic or basic moieties, that leads to increased reactivity in hydrazone exchange.

With this thought in mind, alternative oxygen-containing substrates **1g–i**, and thiophenol **1j** (Fig. 5) were considered computationally as a test of this model, as such substrates contain hydrogen bond acceptors, but lack the suitably acidic/basic groups required to catalyse the reaction *via* intramolecular proton transfer. Amongst these examples, benzoDHP **1g** was predicted to be faster than all the other compounds studied experimentally and was therefore selected for synthesis. The origin of this predicted rate enhancement was clear in the structure of the relevant transition state for **1g** (Fig. 5A). The heterocyclic oxygen atom in this species is positioned in such a way that it can form two stabilizing interactions through a favoured 6-membered ring: one with the protonated hydrazone (2.04 Å, O–H) and a second with the incoming nucleophile (2.73 Å, O–H). Short hydrogen bonding interactions within the transition state indicate stronger stabilizing interactions, the likes of which lower the transition state energy to a greater extent, thus resulting in faster hydrazone exchange. The transition state of benzoDHP **1g** features two such short hydrogen bonds, which are considerably shorter (and therefore presumably stronger) than analogous bond lengths calculated for quinoline **1a** (N–H: 1.96 Å, 3.18 Å) and phenol **1b** (O–H: 2.03 Å, 2.93 Å). This observation suggests that **1g** would offer significantly improved exchange kinetics over quinoline **1a**, an already fast exchanging hydrazone. We then experimentally validated this hypothesis by determining the hydrazone exchange kinetics of benzoDHP **1g** (Fig. 6).

Exchange kinetics of benzoDHP (1g)

Hydrazones **1a**, **1d** and **1g** were exchanged with hydrazide **5** (Fig. 6A) and the kinetics were monitored by ^{1}H NMR spectroscopy and the relative rates of exchange were deduced (see ESI Table S15†). It was necessary to study this exchange process with morpholine hydrazide (**5**) instead of glycol hydrazide **3**, as exchange of **1g** with **3** resulted in product precipitation that convoluted the exchange kinetics (see ESI, Fig. S12†). Gratifyingly, **1g** displayed a 2-fold rate enhancement with respect to quinoline **1a** (Fig. 6B), highlighting the predictive power of our computational model of hydrazone exchange.

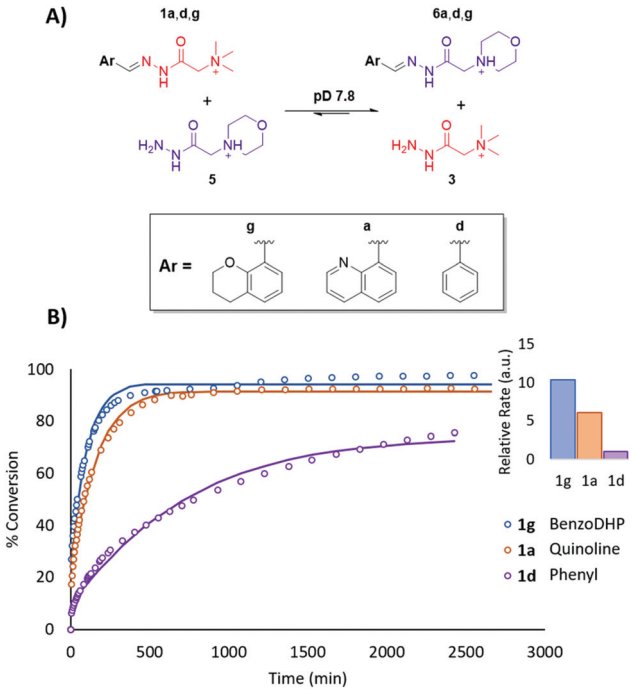

Fig. 6 Hydrazone exchange kinetics of **1a**, **1d** and **1g** were studied at pD 7.8 by ^{1}H NMR spectroscopy. (A) Exchange of hydrazones **1a,d,g** with hydrazide **5**. (B) Kinetic traces of **1a**, **1d**, **1g**. Experimental data and theoretical fit are shown as circles and solid lines, respectively. Inset: Derived relative rates for hydrazone exchange. See ESI† for absolute rate constants.

Despite mechanistic differences between hydrazone exchange and formation processes, we speculate that the rate-enhancing effects observed for proximal acid/base groups upon hydrazone formation may also arise on account of hydrogen bonding interactions which lower the activation energies (by stabilising the transition states). The ability of those groups to facilitate intramolecular proton transfer, as postulated by Kool *et al.*,[6a–d] will also be a contributing factor. Preliminary experiments (ESI, Fig. S16 and S17†) revealed that chroman-8-carbaldehyde (the aldehyde from which benzoDHP **1g** was derived) exhibited rapid hydrazone formation, reacting 15-fold faster than quinoline-8-carbaldehyde, and 26-fold faster than benzaldehyde, which lacks any rate-enhancing features. The intriguing observation that the benzoDHP moiety catalyses rapid hydrazone formation, despite its lack of a significantly acidic or basic group to facilitate intramolecular proton transfer processes, supports our hypothesis that hydrogen-bonding interactions play an important role within the context of organocatalysed hydrazone formation, and probably

also the mechanistically similar processes of imine and oxime formation.

Conclusion

We have demonstrated that the judicial placement of neighbouring hydrogen-bond acceptors within the carbonyl-derived moiety of a hydrazone does lead to enhancements in rates of hydrazone exchange. Computational modelling identified a likely reaction pathway for this process whose energetics were consistent with experimentally determined exchange rates. Modelling supported the hypothesis that the rate-determining step in hydrazone exchange was nucleophilic attack on the protonated hydrazone, which is an important distinction between hydrazone exchange and hydrazone formation, where the rate-limiting step is collapse of the carbinolamine tetrahedral intermediate. Crucially, modelling indicated that the origin of the observed rate enhancements lies in the ability of neighbouring functional groups to form a stabilizing hydrogen bonds within the transition state, and that geometries where 6-membered ring intramolecular hydrogen bonding interactions can be adopted are particularly important. Our confidence in this model was demonstrated by its prediction that a benzoDHP group – containing a very weakly basic but optimally placed oxygen atom that acts as a hydrogen-bond acceptor – displayed fast exchange kinetics, which was gratifyingly supported by experimental observation. Preliminary experiments revealed that chroman-8-carbaldehyde (from which BenzoDHP **1g** was derived) also catalyses rapid hydrazone formation. Surprisingly, chroman-8-carbaldehyde was found to react 15-fold faster than previously reported quinoline-8-carbaldehyde,[6a] despite its lack of an acidic/basic group. These observations suggest that the inclusion of hydrogen-bond acceptor moieties within the aldehyde component may also play an important role in catalysing hydrazone formation, alongside the previously reported[6a–d] catalytic effect of proximal acid/base groups. At neutral pD, benzoDHP **1g** was observed to afford an 2-fold enhancement in the rate of hydrazone exchange, compared to that of quinoline **1a**, and was 10-fold faster than control hydrazone **1d**. With regards to our own interest in dynamic combinatorial chemistry, our work suggests that valuable gains in rate of exchange can be made that would allow the design of a polymer-scaffolded DCLs[12] operating with reasonable kinetics at near-neutral pH – a crucial requirement for interfacing DCLs with biomacromolecules.[13] Furthermore, given the importance of hydrazone exchange within dynamic covalent polymers,[14] materials,[15] surfaces,[16] molecular machines,[17] interlocked molecules,[18] cages[19] and functionalized nanoparticles,[20] where component exchange processes endow structural adaptivity, we speculate this work will offer insight to the design and optimization of new systems. We also anticipate our work will benefit the development of new organocatalysts for hydrazone/oxime formation and exchange processes, indicating that computational studies, on account of their ability to 'pick winners', might minimise tedious preliminary screenings for catalytic activity.

Conflicts of interest

There are no conflicts of interest.

Acknowledgements

The authors wish to thank Dr Rachael Dack (Newcastle University) and Dr Jackie Mosely (Durham University) for assistance with HRMS.

Notes and references

1 (*a*) S. J. Rowan, S. J. Cantrill, G. R. L. Cousins, J. K. M. Sanders and J. F. Stoddart, *Angew. Chem., Int. Ed.*, 2002, **41**, 898–952; (*b*) P. T. Corbett, J. Leclaire, L. Vial, K. R. West, J. L. Wietor, J. K. M. Sanders and S. Otto, *Chem. Rev.*, 2006, **106**, 3652–3711; (*c*) A. Wilson, G. Gasparini and S. Matile, *Chem. Soc. Rev.*, 2014, **43**, 1948–1962.

2 (*a*) Z. Rodriguez-Docampo and S. Otto, *Chem. Commun.*, 2008, **42**, 5301–5303; (*b*) A. Dirksen and P. E. Dawson, *Bioconjugate Chem.*, 2008, **19**, 2543–2548.

3 (*a*) W. P. Jencks, *J. Am. Chem. Soc.*, 1959, **81**, 475–481; (*b*) E. H. Cordes and W. P. Jencks, *J. Am. Chem. Soc.*, 1962, **84**, 832–837; (*c*) E. H. Cordes and W. P. Jencks, *J. Am. Chem. Soc.*, 1962, **84**, 826–831; (*d*) E. H. Cordes and W. P. Jencks, *J. Am. Chem. Soc.*, 1962, **84**, 4319–4328.

4 (*a*) A. Dirksen, S. Dirksen, T. M. Hackeng and P. E. Dawson, *J. Am. Chem. Soc.*, 2006, **128**, 15602–15603; (*b*) A. Dirksen, T. M. Hackeng and P. E. Dawson, *Angew. Chem., Int. Ed.*, 2006, **45**, 7581–7584.

5 B. Shi, R. Stevenson, D. J. Campopiano and M. F. Greaney, *J. Am. Chem. Soc.*, 2006, **128**, 8459–8467.

6 (*a*) E. T. Kool, D. H. Park and P. Crisalli, *J. Am. Chem. Soc.*, 2013, **135**, 17663–17666; (*b*) P. Crisalli and E. T. Kool, *J. Org. Chem.*, 2013, **78**, 1184–1189; (*c*) E. T. Kool, P. Crisalli and K. M. Chan, *Org. Lett.*, 2014, **16**, 1454–1457; (*d*) D. Larsen, M. Pittelkow, S. Karmakar and E. T. Kool, *Org. Lett.*, 2015, **17**, 274–277; (*e*) D. K. Kölmel and E. T. Kool, *Chem. Rev.*, 2017, **117**, 10358–10376; (*f*) L. H. Yuen, N. S. Saxena, H. S. Park, K. Weinberg and E. T. Kool, *ACS Chem. Biol.*, 2016, **11**, 2312–2319; (*g*) D. Larsen, A. M. Kietrys, S. A. Clark, H. S. Park, A. Ekebergh and E. T. Kool, *Chem. Sci.*, 2018, **9**, 5252–5259.

7 H. C. Brown, *et al.*, in *Determination of Organic Structures by Physical Methods*, ed. E. A. Braude and F. C. Nachod, Academic Press, New York, 1955.

8 (*a*) Y. Zhao and D. G. Truhlar, *Theor. Chem. Acc.*, 2008, **120**, 215–241; (*b*) Y. Zhao and D. G. Truhlar, *Acc. Chem. Res.*, 2008, **41**, 157–167.

9 M. J. Frisch, G. W. Trucks, H. B. Schlegel, G. E. Scuseria, M. A. Robb, J. R. Cheeseman, G. Scalmani, V. Barone, B. Mennucci, G. A. Petersson, H. Nakatsuji, M. Caricato, X. Li, H. P. Hratchian, A. F. Izmaylov, J. Bloino, G. Zheng, J. L. Sonnenberg, M. Hada, M. Ehara, K. Toyota, R. Fukuda,

J. Hasegawa, M. Ishida, T. Nakajima, Y. Honda, O. Kitao, H. Nakai, T. Vreven, J. A. Montgomery Jr., J. E. Peralta, F. Ogliaro, M. Bearpark, J. J. Heyd, E. Brothers, K. N. Kudin, V. N. Staroverov, T. Keith, R. Kobayashi, J. Normand, K. Raghavachari, A. Rendell, J. C. Burant, S. S. Iyengar, J. Tomasi, M. Cossi, N. Rega, J. M. Millam, M. Klene, J. E. Knox, J. B. Cross, V. Bakken, C. Adamo, J. Jaramillo, R. Gomperts, R. E. Stratmann, O. Yazyev, A. J. Austin, R. Cammi, C. Pomelli, J. W. Ochterski, R. L. Martin, K. Morokuma, V. G. Zakrzewski, G. A. Voth, P. Salvador, J. J. Dannenberg, S. Dapprich, A. D. Daniels, O. Farkas, J. B. Foresman, J. V. Ortiz, J. Cioslowski and D. J. Fox, *Gaussian 09, Revision C.01*, Gaussian, Inc., Wallingford CT, 2010.

10 (*a*) Y. Lam, M. N. Grayson, M. C. Holland, A. Simon and K. N. Houk, *Acc. Chem. Res.*, 2016, **49**, 750–762; (*b*) R. Wolfenden and M. J. Snider, *Acc. Chem. Res.*, 2001, **34**, 938–945.

11 B. Kuhn, P. Mohr and M. Stahl, *J. Med. Chem.*, 2010, **53**, 2601–2611.

12 (*a*) D. A. Fulton, *Org. Lett.*, 2008, **10**, 3291–3294; (*b*) C. S. Mahon, A. W. Jackson, B. S. Murray and D. A. Fulton, *Chem. Commun.*, 2011, **47**, 7209–7211; (*c*) C. S. Mahon, A. W. Jackson, B. S. Murray and D. A. Fulton, *Polym. Chem.*, 2013, **4**, 368–377.

13 (*a*) A. J. Ruiz-Sanchez, P. L. Higgs, D. T. Peters, A. T. Turley, M. A. Dobson, A. J. North and D. A. Fulton, *ACS Macro Lett.*, 2017, **6**, 903–907; (*b*) C. S. Mahon, M. A. Fascione, C. Sakonsinsiri, T. E. McAllister, W. Bruce Turnbull and D. A. Fulton, *Org. Biomol. Chem.*, 2015, **13**, 2756–2761.

14 (*a*) C. S. Mahon, C. J. McGurk, S. M. D. Watson, M. A. Fascione, C. Sakonsinsiri, W. B. Turnbull and D. A. Fulton, *Angew. Chem., Int. Ed.*, 2017, **56**, 12913–12918; (*b*) C. S. Mahon and D. A. Fulton, *Chem. Sci.*, 2013, **4**, 3661–3666; (*c*) D. E. Whitaker, C. S. Mahon and D. A. Fulton, *Angew. Chem., Int. Ed.*, 2013, **52**, 956–959; (*d*) R. P. Brinkhuis, F. de Graaf, M. B. Hansen, T. R. Visser, F. P. J. T. Rutjes and J. C. M. van Hest, *Polym. Chem.*, 2013, **4**, 1345–1350.

15 (*a*) J. F. Folmer-Andersen and J. M. Lehn, *J. Am. Chem. Soc.*, 2011, **133**, 10966–10973; (*b*) K. S. Kim, H. J. Cho, J. Lee, S. Ha, S. G. Song, S. Kim, W. S. Yun, S. K. Kim, J. Huh and C. Song, *Macromolecules*, 2018, **51**, 8278–8285; (*c*) G. Deng, F. Li, H. Yu, F. Liu, C. Liu, W. Sun, H. Jiang and Y. Chen, *ACS Macro Lett.*, 2012, **1**, 275–279; (*d*) D. D. McKinnon, D. W. Domaille, J. N. Cha and K. S. Anseth, *Chem. Mater.*, 2014, **26**, 2382–2387.

16 (*a*) N. Sakai and S. Matile, *J. Am. Chem. Soc.*, 2011, **133**, 18542–18545; (*b*) P. Charbonnaz, Y. Zhao, R. Turdean, S. Lascano, N. Sakai and S. Matile, *Chem. – Eur. J.*, 2014, **20**, 17143–17151; (*c*) J. Areephong, E. Orentas, N. Sakai and S. Matile, *Chem. Commun.*, 2012, **48**, 10618–10620.

17 (*a*) G. De Bo, S. Kuschel, D. A. Leigh, B. Lewandowski, M. Papmeyer and J. W. Ward, *J. Am. Chem. Soc.*, 2014, **136**, 5811–5814; (*b*) S. Kassem, A. T. L. Lee, D. A. Leigh, A. Markevicius and J. Solà, *Nat. Chem.*, 2016, **8**, 138–143; (*c*) S. Kassem, A. T. L. Lee, D. A. Leigh, V. Marcos, L. I. Palmer and S. Pisano, *Nature*, 2017, **549**, 374–378.

18 (*a*) D. A. Leigh, V. Marcos, T. Nalbantoglu, I. J. Vitorica-Yrezabal, F. T. Yasar and X. Zhu, *J. Am. Chem. Soc.*, 2017, **139**, 7104–7109; (*b*) S. Erbas-cakmak, S. D. P. Fielden, U. Karaca, D. A. Leigh, C. T. Mcternan, D. J. Tetlow and M. R. Wilson, *Science*, 2017, **343**, 340–343.

19 W. Drożdż, C. Bouillon, C. Kotras, S. Richeter, M. Barboiu, S. Clément, A. R. Stefankiewicz and S. Ulrich, *Chem. – Eur. J.*, 2017, **23**, 18010–18018.

20 (*a*) F. Della Sala and E. R. Kay, *Angew. Chem., Int. Ed.*, 2015, **54**, 4187–4191; (*b*) W. Edwards, N. Marro, G. Turner and E. R. Kay, *Chem. Sci.*, 2017, **9**, 125–133.

21 A. Krężel and W. Bal, *J. Inorg. Biochem.*, 2004, **98**, 161–166.